Biochemical Pharmacology 77 (2009) 1348–1357

Contents lists available at ScienceDirect

Biochemical Pharmacology

journal homepage: www.elsevier.com/locate/biochempharm

PARP-1 inhibition-induced activation of PI-3-kinase-Akt pathway promotes resistance to taxol

Arpad Szanto [a,1], Eva E. Hellebrand [b,c,1], Zita Bognar [b], Zsuzsanna Tucsek [b], Aliz Szabo [b], Ferenc Gallyas Jr.[b], Balazs Sumegi [b], Gabor Varbiro [d,*]

[a] Department of Urology, Faculty of Medicine University of Pecs, Pecs, Hungary
[b] Department of Biochemistry and Medical Chemistry, Faculty of Medicine University of Pecs, Pecs, Hungary
[c] Oswestry Dental Centre, Oswestry, Shropshire, UK
[d] Institute for Science and Technology in Medicine, Keele University, Keele, ST5 5BG, Staffordshire, UK

ARTICLE INFO

Article history:
Received 10 November 2008
Accepted 12 January 2009

Keywords:
Antitumor treatment
Taxol resistance
PARP inhibition
Akt activation
PI-3 kinase

ABSTRACT

PARP inhibitors combined with DNA-damage inducing cytostatic agents can lead to effective tumor therapy. However, inhibition of poly(ADP-ribose) polymerase (PARP-1; EC 2.4.2.30) induces the activation of PI-3-kinase-Akt pathway, which can counteract the effectiveness of this therapy. To understand the role of Akt activation in the combined use of cytostatic agent and PARP inhibition, we used taxol (paclitaxel) as an antineoplastic agent, which targets microtubules and up-regulates mitochondrial ROS production, together with (i) pharmacological inhibition (PJ-34), (ii) siRNA knock-down and (iii) transdominant expression of the DNA binding domain of PARP-1. In all cases, PARP-1 inhibition leads to suppressed poly-ADP-ribosylation of nuclear proteins, prevention of NAD^+ depletion and significant resistance against taxol induced caspase-3 activation and apoptotic cell death. Paclitaxel induced a moderate increase in Akt activation, which was significantly augmented by PARP inhibition, suggesting that PARP inhibition-induced Akt activation could be responsible for the cytostatic resistance. When activation of the PI-3-kinase-Akt pathway was prevented by LY-294002 or Akt Inhibitor IV, the cytoprotective effect of PARP inhibition was significantly diminished showing that the activation of PI-3-kinase-Akt cascade had significantly contributed to the cytostatic resistance. Our study demonstrates that drug-induced drug resistance can be responsible for the reduced efficacy of antitumor treatment. Although inhibition of PARP-1 can promote cell death in tumor cells by the inhibition of DNA repair, PARP-inhibition promoted activation of the PI-3-kinase-Akt pathway can counteract this facilitating effect, and can cause cytostatic resistance. We suggest augmenting PARP inhibition by the inhibition of the PI-3-kinase-Akt pathway for antitumor therapy.

1. Introduction

The nuclear enzyme poly(ADP-ribose) polymerase-1 (PARP-1) is activated in response to DNA damage [1]. Single- and/or double-strand DNA breaks induce the production of branched chain ADP-ribose polymers that are covalently attached to numerous nuclear proteins like histones or the PARP itself and this process represents an early event in DNA repair. Although it is well-documented that inhibition of PARP-1 has cytoprotective effects against oxidative stress [2], there is growing evidence suggesting that inhibition of PARP-1 sensitizes cells to DNA-damaging agents [3]. This later effect of PARP-1 inhibition is attributed to the DNA-damage sensing function of PARP-1, namely that it responds to single- and/or double-strand DNA breaks, and facilitates DNA repair and cell survival. Furthermore, it was shown that cells deficient in breast cancer associated gene-1 and -2 (BRCA1/2) are extremely sensitive to PARP inhibition because of defective double-strand DNA break repair [4]. Based on these data, PARP inhibition is considered as a useful therapeutic strategy not only for the treatment of BRCA mutation-associated tumors, but also for the treatment of a wider range of tumors bearing a variety of deficiencies in the homologous recombination DNA repair pathway [5]. However, it has also been shown that inhibition of PARP leads to phosphorylation, and thus activation, of Akt in various tissues [6–8]. It raises the possibility that application of PARP inhibitors in tumor therapy may activate the phosphatidylinositol-3 kinase (PI-3K)-Akt pathway, which initiates processes like

* Corresponding author. Tel.: +44 1782 733 877; fax: +44 1782 583 326.
E-mail addresses: g.varbiro@keele.ac.uk, varbiro@btinternet.com (G. Varbiro).
[1] The first two authors contributed equally to this work.

Abbreviations: PARP, poly(ADP-ribose) polymerase; PAR, poly(ADP-ribose); PI-3K, phosphatidylinositol-3-kinase; Akt/PKB, protein kinase B; MTT^+, 3-[4, 5-dimethylthiazol-2-yl]-2, 5-diphenyl-tetrazolium bromide.

0006-2952/$ – see front matter © 2009 Elsevier Inc. All rights reserved.
doi:10.1016/j.bcp.2009.01.008

the inactivation of glycogen synthase kinase-3, caspase-9, Bad or forkhead homolog rhabdomyosarcoma (FKHR) transcription factors [9] leading to cytostatic resistance.

Paclitaxel (taxol) interferes with the mitotic spindle during mitosis of cells, stabilizing the microtubule by inhibiting tubulin dimerisation and so inhibiting the separation of the sister chromatids [10–12]. Paclitaxel can affect kinases [13] that play important roles in cell death processes, and regulate the expression of tumor suppressor genes and cytokines [14]. In addition, paclitaxel can induce cytosolic calcium oscillations [15] and mitochondrial permeability transition, as well as elevated generation of reactive oxygen species predominantly at cytochrome oxidase in tumor cells [16]. In the paclitaxel-induced cell death process, activation of c-Jun N-terminal kinase (JNK) plays a critical role by suppressing Akt activation and promoting the nuclear accumulation of forkhead-related transcription factor-3a (Foxo3a; [17]). Nuclear translocation of Foxo3a can facilitate apoptosis by inducing the expression of Bim, a BH3-only proapoptotic bcl-2 homolog protein [18]. It has also been demonstrated that Akt overexpression prevented paclitaxel-induced cell death [19–23], probably by a mechanism involving Akt dependent phosphorylation of FOXOs that stabilizes their binding to cytosolic 14-3-3 protein and so prevents their translocation to the nucleus, resulting in inhibition of transcription of FOXO dependent genes such as Bim [24].

In the present paper, we provide evidence that inhibition of PARP-1 activity can indeed cause resistance to paclitaxel-induced death in tumor cells, and activation of the PI-3K-Akt pathway is significantly involved in this effect.

2. Material and methods

2.1. Materials

Taxol (paclitaxel) was from ICN Biomedicals Inc. (Aurora, OH), Verapamil was from Richter Gedeon Rt. (Budapest, Hungary), PI3 kinase inhibitor LY-294002, PARP-1 inhibitor PJ-34, protease inhibitor cocktail, and all the chemicals for cell culture were purchased from Sigma–Aldrich Kft (Budapest, Hungary). InSolution Akt Inhibitor IV was from Calbiochem (Darmstadt, Germany) The following antibodies were used: anti-Akt, anti-phospho-Akt, anti-glycogen synthase kinase-3β (GSK), anti-phospho-glycogen synthase kinase-3β (GSK), anti-JNK, anti-phospho-c-Jun N terminal kinase (JNK), anti-p38 MAPK, anti-phospho-p38 mitogen activated protein kinase (p38 MAPK) and anti-p44/42 MAPK (Erk1/2), (Cell Signalling Technology, Beverly, MA); anti-phospho-extracellular signal regulated kinase (Erk1/2) anti-PAR and anti PARP (Alexis Biotechnology, London, UK); anti-glyceraldehyde-3-phosphate dehydrogenase (GAPD, Delta Biolabs, Gilroy, CA); anti-mouse IgG and anti-rabbit IgG (Sigma–Aldrich Kft, Budapest, Hungary).

2.2. Cell culture

Hela human cervical cancer and T24 human bladder carcinoma cells were from American Type Culture Collection (Wesel, Germany). The cells were maintained as monolayer adherent culture in Minimum Essential Eagle's Medium containing 1% antibiotic–antimycotic solution (Sigma–Aldrich Kft Budapest, Hungary) and 10% fetal calf serum (MEM/FCS) in humid 5% CO_2 atmosphere at 37 °C.

2.3. Transdominant expression of DNA-binding domain of PARP

The coding region of the N-terminal DNA-binding domain (DBD) of PARP (PARP-N214, AA residues 1-214) [25] was amplified by PCR and cloned in-frame into pEGFP-C1/N3 vectors (Clontech, Palo Alto, CA) after cutting with HindIII and EcoRI restriction enzymes (Fermentase, Vilnius, Lithuania). For enabling active nuclear transport of the GFP tagged PARP-N214, the nuclear localization signal (NLS) was added to the N-terminal of PARP-N214 sequence using PCR primers coding the NLS sequence. The recombinant pPARPGFP-C1/N3 vectors were purified by a plasmid purification kit (Qiagen, Valencia, CA) and utilized for transient transfection of T24 and HeLa cells by using Lipofectamine2000 (Invitrogen, Frederick, MD) according to the manufacturers' protocol. For effective transdominant expression of PARP-DBD, the transfection step was repeated 48 h after the first transfection, and the experiments on the cells were performed 40 h after the second transfection [8].

2.4. Suppression of PARP-1 expression by small interfering RNA (siRNA) technique

The cells were transiently transfected with siRNA designed for PARP-suppression by the manufacturer (Santa Cruz Biotechnology, Santa Cruz, CA) in Opti-MEM® I Reduced Serum Medium (Gibco, Brooklyn, NY) using Lipofectamin2000 (Invitrogen, Frederick, MD). For effective suppression of PARP, the transfection step was repeated twice with 48 h interval between the transfections, and the experiments on the cells were performed 40 h after the third transfection [8].

2.5. Cell viability assay

The cells were seeded into 96-well plates at a starting density of 10^4 cells per well and cultured overnight before paclitaxel and PJ-34 or different protein kinase inhibitors were added to the medium at the concentration and composition indicated in the figure legends. After 24 h of treatment, the medium was removed and fresh MEM/FCS containing 0.5% of the water soluble yellow mitochondrial dye, 3-[4,5-dimethylthiazol-2-yl]-2,5-diphenyl–tetrazolium bromide (MTT^+; Sigma–Aldrich Kft, Budapest, Hungary) was added. Incubation was continued for an additional 3 h, and the MTT^+ reaction was terminated by adding HCl to the medium to a final concentration of 10 mM. The amount of water-insoluble blue formasan dye formed from MTT^+ was proportional to the number of live cells, and was determined with an Anthos Labtech 2010 ELISA reader (Vienna, Austria) at 550 nm wavelength after dissolving the blue formasan precipitate in 10% sodium dodecyl sulfate. All experiments were run with at least four replicate cultures and repeated three times [26,27].

2.6. Determination of paclitaxel uptake

One million/well T24 cells were seeded to 6-well plates and incubated for 3 h in the presence of 10, 100 or 1000 nM paclitaxel only, or together with 10 μM PJ-34 and/or 40 μM verapamil. After the incubation, the cells were harvested, and homogenized by sonication. Paclitaxel content of the samples was determined by high-pressure liquid chromatography and mass spectrometry (HPLC–MS) after deproteinization by perchloric acid. For the separation, an isocratic method was applied using 5 mM sodium acetate, pH 4.5 – acetonitrile 50:50 (v/v) mixture as solvent at a flow rate of 1.2 ml/min. The same HPLC system that was used for cytochrome *c* measurement was connected to a Bruker HCT Esquire (Bruker Daltonics, Bremen, Germany) MS instrument through a microsplitter valve (Upchurch Scientific, Oak Harbor, WA), the flow rate was 1.2 ml/min with a splitting ratio of 7 over 3. The electrospray ion source was operated in positive mode. Nitrogen was used as drying gas at 250 °C, with a flow rate of 8 l/min, the pressure of the nebulizer was set at 12 psi. We used the Smart Parameter Setting (SPS) with target mass of 854 *m/z* (wide

range). The scanning mass to charge range was 50–2000 m/z with a scanning speed of 8100 m/z/s. Maximum accumulation time was 200 ms. For control of the instrument, the Esquire Control Version 5.3 Build 11, and for data evaluation the Data Analysis Version 3.3 Build 146 software was used (Bruker Daltonics, Bremen, Germany). Quantization was carried out using peak areas method. Results are expressed as pmole paclitaxel/mg protein, mean ± S.E.M. of three independent experiments.

2.7. Determination of NAD^+

Cells were treated with paclitaxel and PJ-34 as for the cell viability assay using three replicate cultures and each experiment was repeated twice. The NAD^+ level was measured exactly as described previously [8]. Briefly, cells were cultured in a 96-well plate and treated with paclitaxel in the presence or absence of PJ-34 and PI-3K inhibitor LY-294002 as described. Cellular NAD^+ levels were measured by the microplate version of the enzymatic cycling method using alcohol dehydrogenase exactly as described [28]. The reaction was monitored at 550 nm and was allowed to run for 10 min. A standard curve was generated using known concentrations of NAD^+ for the calculation of the cellular NAD^+ levels.

2.8. Western blot analysis

The cells were seeded and treated as for the cell viability assay. After the time indicated, the cells were harvested in a chilled lysis buffer containing 0.5 mM sodium-metavanadate, 1 mM EDTA and protease inhibitor cocktail in PBS. The proteins were precipitated with TCA, washed three times with −20 °C acetone and subjected to sodium dodecylsulfate polyacrylamide gel electrophoresis. Proteins (20 μg per lane) were separated on 12% gels then transferred to nitrocellulose membranes. The membranes were blocked in 5% low-fat milk for 1 h at room temperature then exposed to the primary antibodies at 4 °C overnight at a dilution of 1:1000 in blocking solution. Appropriate horseradish peroxidase-conjugated secondary antibodies were used for 3 h at room temperature at a dilution of 1:5000. Peroxidase labeling was visualized with enhanced chemiluminescence labeling using an ECL Western blotting detection system (Amersham Biosciences, Budapest, Hungary). The developed films were scanned and the pixel volumes of the bands were determined by using NIH's Image J software. All experiments were repeated three times [29].

2.9. Caspase-3 activity assay

Caspase-3 activity following paclitaxel administration in the presence or absence of the PARP inhibitor PJ-34 was carried out exactly as described previously [30]. Briefly, the cells were treated with paclitaxel in the presence or absence of PJ-34 for the time indicated. The cells were harvested, washed twice in PBS and resuspended in a cell lysis buffer. Forty micrograms of protein were incubated with 50 μM of fluorescent caspase substrate Ac-DEVD-AMC (Sigma–Aldrich Kft Budapest, Hungary) in four parallels for 3 h. Fluorescence was detected by a fluorescent ELISA plate reader at the excitation and emission wavelength of 360 nm and 460 nm, respectively.

2.10. Determination of cytochrome c level by HPLC method

The analysis of cyt-*c* from the cytosol fraction of T24 or HeLa cells treated with paclitaxel in the presence or absence of PJ-34 for 18 h was performed on a non-porous 33 mm × 4.6 mm KOVASIL-MS C18 column (Zeochem AG, Uetikon, Switzerland). Measurements were performed on a Dionex HPLC system consisting of a Dionex P 580 low pressure gradient pump, a Dionex UVD 340S diode array detector (chromatograms were detected at 393 nm) and a Rheodyne 8125 injector equipped with a 20 μl loop. Instrument control and data acquisition were carried out using Chromeleon data management software. The following gradient was used at a 1 ml/min flow rate; eluent A consisted of 10:90 acetonitrile–water +0.1% (v/v) trifluoroacetic acid and eluent B consisted of 90:10 acetonitrile–water +0.1% (v/v) trifluoroacetic acid; 0 → 7 min: from 0% B to 70% B, 7 → min 12: from 70% B to 100% B, 12 → 12.5 min: from 100% B to 0% B, 12.5 → 14.5 min: 0% B. Data acquisition was performed from at least three independent experiments.

2.11. Statistical analysis

Data were presented as means ± S.E.M. For multiple comparisons of groups, ANOVA was used. Statistical difference between groups was established by paired or unpaired Student's *t*-test, with Bonferroni's correction.

3. Results

3.1. PARP inhibition induces paclitaxel-resistance in tumor cell lines

Exposing wild type or T24 bladder carcinoma (Fig. 1) or HeLa cervix tumor (data not shown) cells to 100 nM of paclitaxel induced a massive increase in poly(ADP-ribosylation) of nuclear proteins that reached its maximum in about 3 h and did not change significantly further on (Fig. 1A). When the wild type T24 bladder carcinoma cells were pre-treated with 10 μM of PJ-34 (31), an effective inhibitor of PARP-1, 30 min prior to the administration of paclitaxel, no ADP-ribosylation of the nuclear proteins was detected (Fig. 1B). When the cells were mock transfected or transfected with a construct expressing DNA binding domain of PARP-1 (PARP-DBD; 8) or siRNA designed for the suppression of PARP protein expression at the translational level (8), paclitaxel-induced ADP-ribosylation was also abolished in the cells transfected with construct expressing DNA binding domain of PARP-1 or transfected with siRNA (Fig. 1C) exactly as observed in the case of wild type cells treated with PJ-34 (Fig. 1B). Similar results were obtained using HeLa cells (data not shown). These data show that paclitaxel treatment resulted in a massive activation of PARP-1 activity that was effectively prevented by all the three methods used for suppression of the catalytic activity of the enzyme.

Under our experimental conditions, 12 h or longer exposure to 100 nM paclitaxel significantly decreased the viability ($p < 0.01$) of T24 (Fig. 2A) and HeLa cells (data not shown). However, when 10 μM PJ-34 was added to the medium 30 min before the application of paclitaxel, the effect of the drug on cell viabilities was significantly attenuated ($p < 0.01$) indicating that the PARP inhibitor provided protection against paclitaxel in the cancer cell lines studied (Fig. 2A). In order to reveal whether the observed paclitaxel-resistance was due to any interference with ABC transporters, we blocked P-glycoprotein pathway by 40 μM verapamil. Co-treating the cells with verapamil and PJ-34 significantly reduced the viability of both tumor cell lines even in the absence of paclitaxel, while verapamil by itself caused a slight, statistically non-significant decrease in the viabilities of both T24 cells (Fig. 2B) and Hela cells (Fig. 2C). Verapamil indeed enhanced the effect of paclitaxel in both cell lines, so in the presence of verapamil, maximal effect of paclitaxel was observed at 10 rather than 1000 nM concentration. On the other hand, PJ-34 desensitized T24 and HeLa cells towards paclitaxel, and increased cell viability at all paclitaxel concentrations (Fig. 2B and C). The fact that at higher paclitaxel concentrations verapamil did not interfere with the desensitizing effect of PJ-34 suggests that the PARP

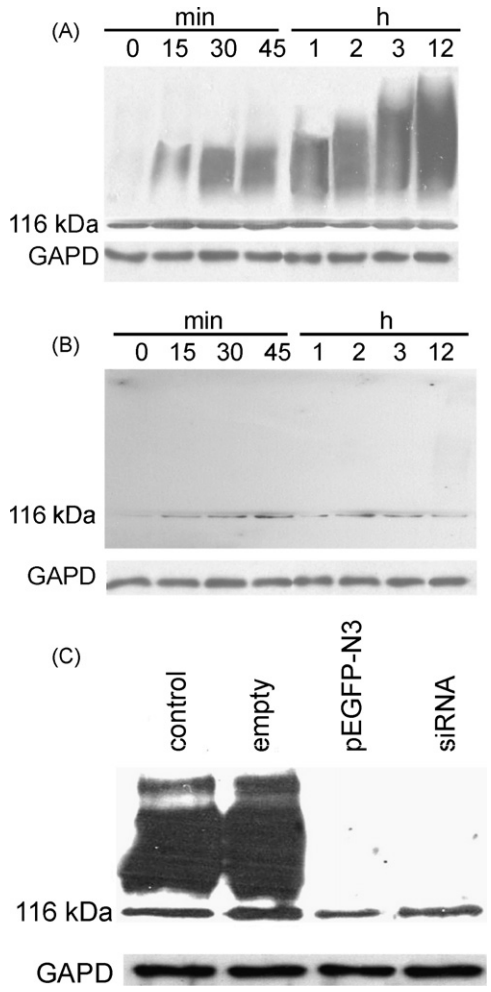

Fig. 1. Effect of PARP inhibition on paclitaxel-induced ADP-ribosylation. In (A) wild type (wt) T24 cells were exposed to 100 nM of paclitaxel for the indicated time. In (B) wild type (wt) T24 cells were pretreated with 10 μM of PJ-34 prior to the exposure to 100 nM of paclitaxel for the indicated time. In (C) wild type (wt: control), mock transfected (empty), PARP-DBD expressing (pEGFP-N3) and PARP-siRNA transfected (siRNA) T24 cells were exposed to 100 nM of paclitaxel for 3 h. Equal amounts of proteins were separated by SDS-PAGE and the protein poly (ADP)-ribosylation was detected by Western blotting utilizing an anti-ADP-ribose antibody. Gliceraldehyde-3-phosphate dehydrogenase (GAPD) was used as a loading control. Results are presented as representative blots of three independent experiments.

inhibition evoked drug resistance in tumor cells was not likely to be related to ABC transporter mechanisms.

We approached the question of the interference between the PARP inhibitor and the ABC transporter more directly by determining the amount of paclitaxel taken up by T24 cells during 3 h incubation in the presence of 10, 100 and 1000 nM of paclitaxel alone or together with 10 μM PJ-34 and/or 40 μM verapamil. As shown in Table 1 the PARP inhibitor slightly, although not significantly, decreased paclitaxel uptake, while verapamil very significantly increased it, regardless of the presence or absence of PJ-34. This result confirmed that the PARP inhibition-induced paclitaxel resistance by an alternative mechanism, and not by interacting with ABC transporter systems.

3.2. Transdominant expression of DNA-binding domain of PARP

To demonstrate that the inhibition of nuclear PARP-1 and not a side effect of the pharmacological PARP inhibitor was indeed responsible for the paclitaxel-resistance, we assessed the effect of non-pharmacological PARP inhibition on paclitaxel-induced cell death. We transiently transfected T24 bladder carcinoma cells with a construct (pEGFP-N3) expressing a fusion protein consisting of the nuclear localization signal and the DNA-binding domain of PARP attached to the N terminus of green fluorescent protein (GFP). Control cells were transfected with the same construct expressing only the GFP. While latter protein was localized in the cytosol, the hybrid protein with the nuclear localization signal was localized to the nucleus as detected by fluorescent microscopy (data not shown). No significant difference between the viability of cells either non-transfected or mock transfected (GFP-expressing only) was detected in response to paclitaxel administration (Fig. 3A). When the cells were transfected with the plasmid expressing the hybrid protein, the paclitaxel-induced cytotoxicity was significantly lower ($p < 0.01$) when compared to non-transfected control cells (Fig. 3A). Similar results were detected in the HeLa cell line (data not shown).

Table 1
Effect of PJ-34 and verapamil on paclitaxel uptake of T24 cells. Paclitaxel concentration in the cells were determined by HPLC–MS after incubating them for 3 h in the presence of 10, 100 or 1000 nM paclitaxel only, or together with 10 μM PJ-34 and/or 40 μM verapamil.

Paclitaxel	10 nM	100 nM	1000 nM
Alone	14.0 ± 5.2	47.2 ± 6.8	185.8 ± 32.2
With PJ-34	6.3 ± 2.4	40.2 ± 8.3	175.1 ± 27.9
With verapamil	299.1 ± 41.8	590.7 ± 68.6	1610.6 ± 121.5
With verapamil and PJ-34	166.3 ± 39.7	526.4 ± 75.1	1491.8 ± 144.1

Results are expressed as pmole paclitaxel/mg protein, means ± S.E.M. of three independent experiments.

3.3. Suppression of PARP expression by RNA-interference

PARP inhibition was also achieved by suppressing its expression with RNA interference. T24 bladder carcinoma cells were transfected with PARP siRNA in accordance with the manufacturer's recommendations. The knock-down of PARP was verified by Western blotting (data not shown). Following 24 h of paclitaxel treatment, no significant difference was detected between the control and siRNA transfected cells up to the paclitaxel concentration of 10 nM. However above this concentration, the viability of siRNA transfected cells was significantly higher ($p < 0.01$) when compared to controls (Fig. 3B). We obtained similar results in the HeLa cell line (data not shown).

3.4. PARP inhibition decreases the paclitaxel-induced caspase-3 activation

According to previous studies, paclitaxel administration induces mainly apoptotic cell death, so we tested caspase-3 activation and cytochrome *c* release in our experimental setup. In T24 bladder carcinoma cells, 12 h of paclitaxel treatment at the concentration of 100 and 1000 nM resulted in marked activation of caspase-3 (Fig. 4A), and this effect was significantly reduced ($p < 0.01$) when the cells were pretreated with 10 μM of PJ-34 (Fig. 4A). The time-course for the activation of caspase-3 by paclitaxel was also investigated. The administration of paclitaxel at the concentration of 100 nM induced a significant increase in caspase-3 activity ($p < 0.05$) in T24 bladder carcinoma cells after 3 h when compared to untreated control (Fig. 4B). When the cells were pretreated with 10 μM of PJ-34, the level of caspase-3 activation was significantly lower compared to the cells that were treated solely with paclitaxel. Similar results were obtained with HeLa cells (data not shown). Mitochondrial cytochrome *c* release was determined by a quantitative HPLC method. In T24 cells, 12 h of 100 nM paclitaxel treatment resulted in an increased release of cytochrome *c*. When the cells were pretreated with 10 μM PJ-34, this effect was

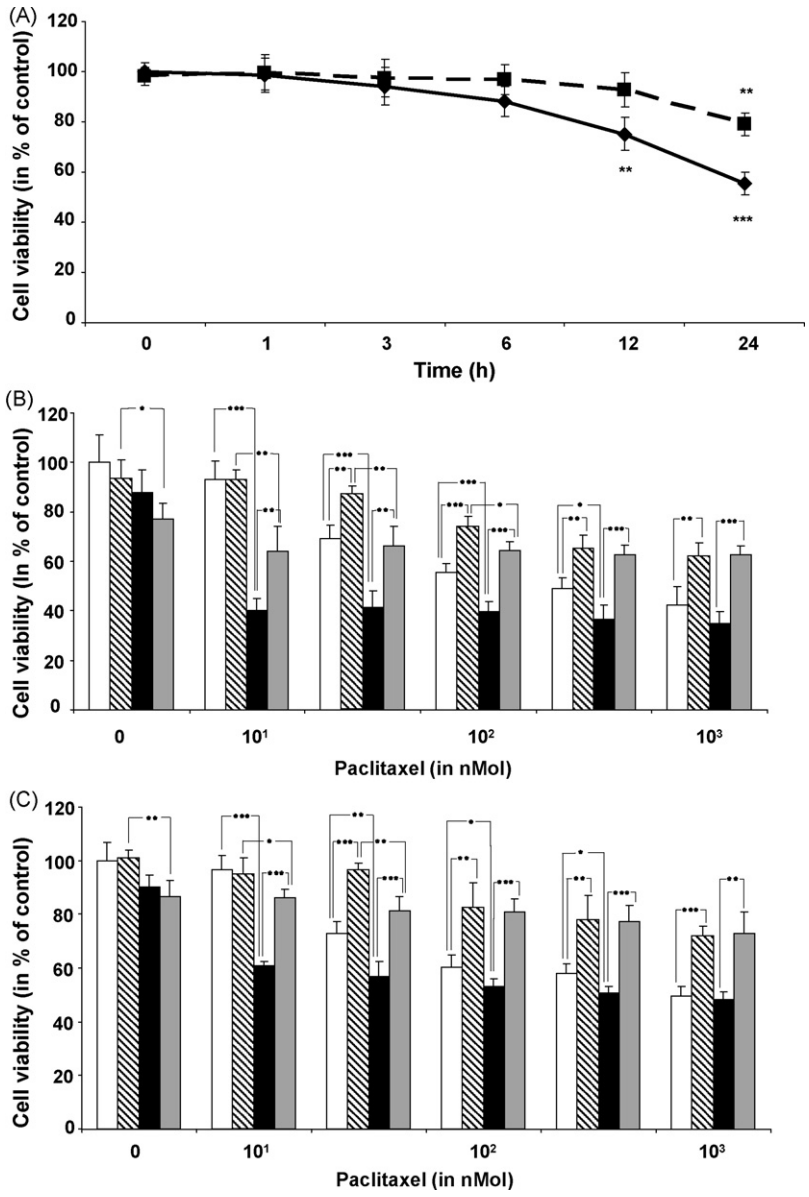

Fig. 2. Effect of paclitaxel, PJ-34 and verapamil on the viability of cell lines. In (A) the effect of 100 nM of paclitaxel in the absence (solid line) or presence of 10 μM of PJ-34 (broken line) on the time-course of the viability of T24 cells, which was detected by the formation of water-insoluble formasan dye from the yellow mitochondrial dye MTT^+ by the functionally active mitochondria of the cells. Data represent mean ± S.E.M. of three independent experiments, each using four replicate cultures. Note that the concentration axis is logarithmical. Significance shown below the solid line indicates difference from untreated cells, while the one above the broken line means difference from the cells treated with equimolar paclitaxel only. In (B) the effect of verapamil on the viability of T24 cells was also detected by the MTT^+ method. The cells were exposed for 24 h to different concentrations of paclitaxel either alone (empty bars) or pretreated with 10 μM of PJ-34 (striped bars), pretreated with 40 μM of verapamil (filled bars) or pretreated with 10 μM of PJ-34 and 40 μM of verapamil (grey bars) 30 min prior to the paclitaxel administration. In (C) the effect of verapamil on the viability of HeLa cells was also detected by the MTT^+ method. The cells were exposed for 24 h to different concentrations of paclitaxel either alone (empty bars) or pretreated with 10 μM of PJ-34 (striped bars), pretreated with 40 μM of verapamil (filled bars) or pretreated with 10 μM of PJ-34 and 40 μM of verapamil (grey bars) 30 min prior to the paclitaxel administration. Data represent mean ± S.E.M. of three independent experiments, each using four replicate cultures. Note that the concentration axis is logarithmical. *, significant difference ($p < 0.05$); **, significant difference ($p < 0.01$); ***, significant difference ($p < 0.001$).

significantly reduced ($p < 0.01$). Furthermore, 5 μM of LY294002 significantly enhanced cytochrome *c* release induced by paclitaxel ($p < 0.01$) and diminished the reducing effect of PJ-34. Similar results were obtained in case of the HeLa cells (data not shown).

3.5. PARP inhibition leads to the activation of Akt/PKB

To elucidate the role of the nuclear enzyme PARP-1 in regulating the proteomic signal transduction pathway, we analyzed activation of Akt/protein kinase B, Erk, JNK and p38 MAP kinases in response to paclitaxel treatment in the presence of PJ-34 in T24 bladder carcinoma cells. Previously, we observed Akt activation as soon as 15 min after PJ-34 treatment, so we assessed the levels of kinases up to 3 h following 100 nM of paclitaxel administration in the presence or absence of 10 μM of PJ-34.

The level of total Akt was unaltered in response to either paclitaxel or PJ-34 administration (Fig. 5). Paclitaxel administration resulted in a slightly increased Akt (Ser^{473}) phosphorylation after only 3 h. However, it increased within 15 min of PJ-34 administration, and the increased level was maintained throughout the observation period (Fig. 5). The total level of glycogen synthase kinase-3β (GSK-3β), the downstream target of Akt, was not altered in response to either paclitaxel or PJ-34 administration (Fig. 5). However the phosphorylation of GSK-3β presented a

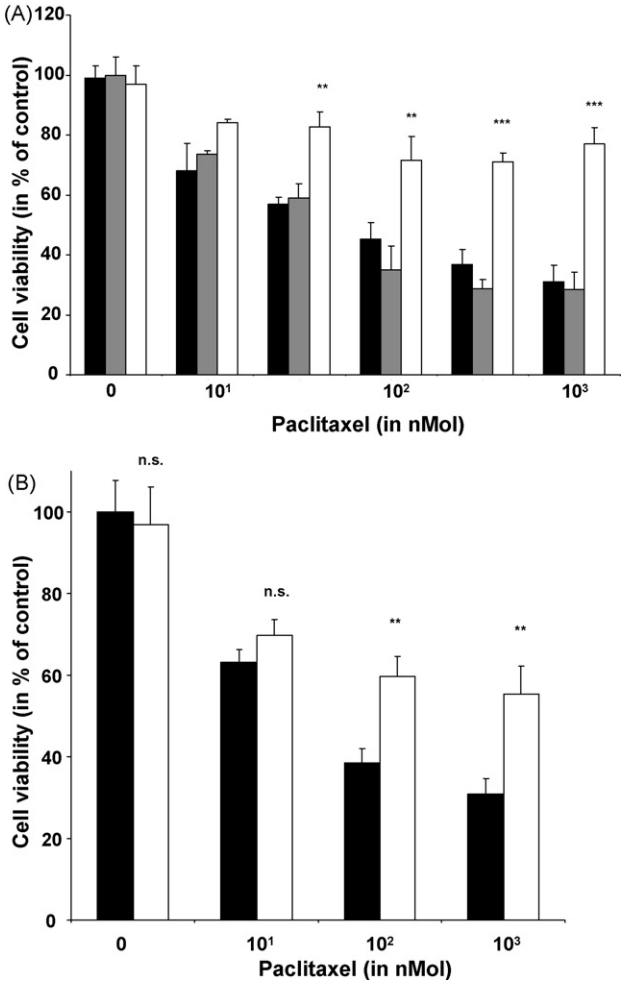

Fig. 3. Effect of non-pharmacological PARP inhibition on cell viability. In (A) wild type (filled bars), mock transfected (gray bars) and PARP-DBD expressing (empty bars) T24 cells were exposed to different concentrations of paclitaxel for 24 h. The viability was detected by the MTT$^+$ method. Data represent mean ± S.E.M. of three independent experiments running in four parallels. Note that the concentration axis is logarithmical. **, significant difference ($p < 0.01$) between transfected and mock transfected cells exposed to equimolar concentration of paclitaxel. In (B) T24 cells were either untransfected (empty bars) or transfected with PARP siRNA (filled bars) in accordance with the recommendations of the manufacturer and were exposed to different concentrations of paclitaxel for 24 h. Viability was monitored using the MTT$^+$ method. Data represent mean ± S.E.M. of three independent experiments, each using four replicate cultures. Note that the concentration axis is logarithmical. **, significant difference ($p < 0.01$) between PARP knock-down and wild type cells exposed to equimolar concentrations of paclitaxel.

similar pattern to Akt, showing increased phosphorylation 30 min after paclitaxel and PJ-34 co-administration and slightly increased phosphorylation after 3 h in the absence of PJ-34 (Fig. 5). Contrary to phospho-Akt, neither paclitaxel nor PJ-34 administration influenced the level of phosphorylated p38 or Erk1/2. Paclitaxel treatment increased JNK activation, however, pretreatment with 10 μM of PJ-34 failed to modify this effect (Fig. 5). When we determined the total MAP kinase levels (Erk1/2, p-38 and JNK, respectively), no alteration was detected up to 3 h following 100 nM of paclitaxel administration in the presence or absence of 10 μM of PJ-34.

3.6. Inhibition of the PI-3K/Akt pathway diminishes paclitaxel resistance induced by inhibition of PARP

Since PARP inhibition leads to the activation of the Akt/PKB-GSK-3β pathway and also to paclitaxel resistance, it seemed

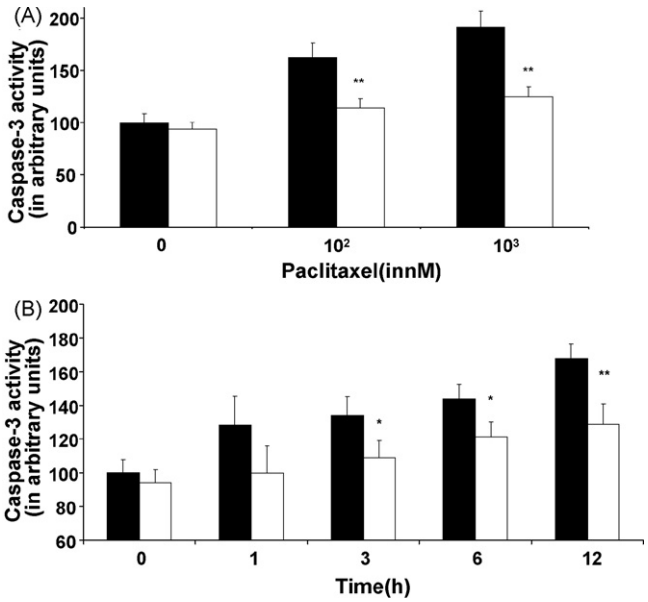

Fig. 4. Effect of paclitaxel and PJ-34 on the activity of caspase-3 in T24 cells. Cytosolic fraction of cells untreated (filled bars) or pretreated with 10 μM of PJ-34 (empty bars) were exposed to different concentrations of paclitaxel for 12 h (A) or were exposed to 100 nM of paclitaxel for different times (B). Caspase-3 activity was detected by a fluorescent plate reader using the fluorescent substrate Ac-DEVD-AMC. Data represent mean ± S.E.M. of three independent experiments, each using four replicate cultures. *, significant difference ($p < 0.05$); **, significant difference ($p < 0.01$) between cells pretreated and not with PJ-34 and exposed to equimolar concentrations of paclitaxel.

reasonable to investigate whether the paclitaxel resistance was mediated by Akt activation. To this end, we inhibited Akt by two different inhibitors, and determined the effect of PARP inhibition on paclitaxel-induced cell death under these conditions. Five

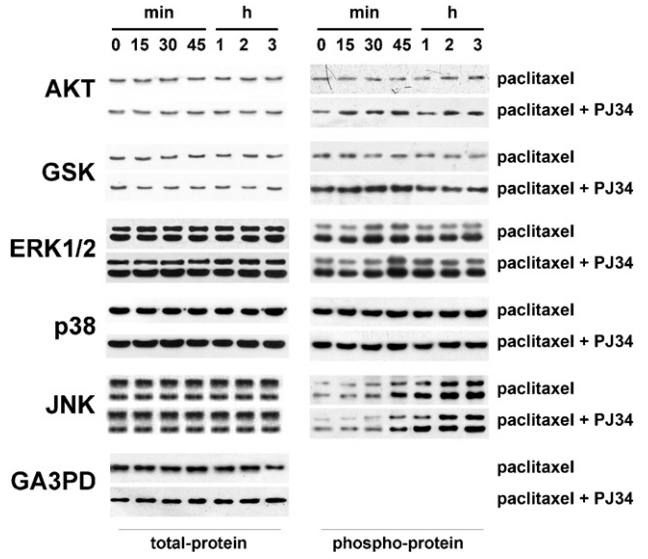

Fig. 5. Effect of paclitaxel and PJ-34 on the activation of various intracellular protein kinases. T24 cells were treated with either 100 nM of paclitaxel alone or pretreated with 10 μM of PJ-34 for the indicated times. Total cell extracts were separated by SDS-PAGE and the activation of Akt (p-AKT), GSK-3β (p-GSK), p44/42 MAPK Erk1/2 (p-ERK1/2), p38 MAPK (p-P38) and JNK (p-JNK) was detected with phosphorylation specific antibodies. The level of total Akt, GSK-3β, p44/42 MAPK Erk1/2, p-38 and JNK in T24 cell treated with either 100 nM of paclitaxel alone or pretreated with 10 μM of PJ-34 30 min prior to paclitaxel administration for the indicated times was also detected by specific antibodies. Even protein loading was confirmed by anti-GA3PD antibody and Western blotting. Representative blots of three independent experiments.

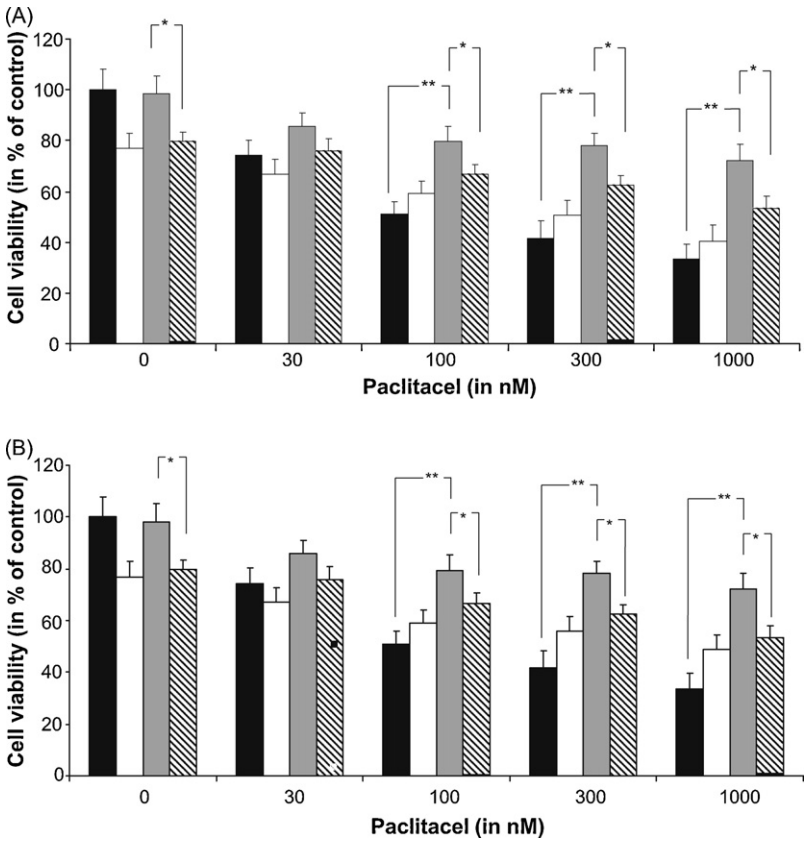

Fig. 6. Effect of PI3-K/Akt pathway inhibition on the PARP inhibition-induced paclitaxel resistance. In (A) T24 cells were exposed for 24 h to different concentrations of paclitaxel alone (filled bars) or pretreated with 5 μM of LY-294002 (empty bars), with of 10 μM of PJ-34 (gray bars) or with the combination of PJ-34 and LY-294002 (striped bars). In (B) in an identical experimental setup, LY-294002 was replaced with 5 μM of Akt Inhibitor IV alone (empty bars) or in combination with PJ-34 (striped bars). Viability of the cells was detected by the MTT$^+$ method. Data represent mean ± S.E.M. of three independent experiments, each using four replicate cultures. Note that the concentration axis is logarithmical. *, significant difference ($p < 0.05$); **, significant difference ($p < 0.01$) between cells treated with exposure to equimolar concentration of paclitaxel in the presence of PJ-34 alone and together with the Akt inhibitor.

micromolars of the PI-3K inhibitor LY-294002 decreased viability of T24 cells by about 20% when applied alone, and significantly decreased paclitaxel resistance caused by PJ-34 (Fig. 6A). When Akt/PKB was inhibited by a different inhibitor, Akt Inhibitor IV, viability of T24 cells was reduced by about 30% when the drug was applied alone, and decreased paclitaxel resistance caused by PARP inhibition more effectively than LY-294002 did (Fig. 6B). Similar results were obtained in the case of Hela cells (data not shown). These results suggest that paclitaxel resistance induced by PARP inhibition was indeed mediated by Akt activation in a significant extent.

3.7. PARP inhibition but not the inhibition of Akt influences the intracellular level of NAD$^+$

Paclitaxel treatment leads to protein poly(ADP-ribosylation) as detected by Western blotting (Fig. 1A). Since the ADP-ribose polymers are synthesized by PARP using NAD$^+$ as its substrate and resynthesis of NAD$^+$ is energetically costly, PARP inhibition could cause paclitaxel resistance by relieving this metabolic burden. To address this issue, we measured intracellular NAD$^+$ levels following paclitaxel administration either alone or in combination with PJ-34 and LY-294002 or Akt inhibitor IV. T24 cells were treated with paclitaxel at the concentration of either 100 nM or 1000 nM for 24 h. This leads to the activation of PARP and the decrease of intracellular NAD$^+$ level. When the cells were pretreated with 10 μM of PJ-34 for 30 min prior to the administration of paclitaxel, the level of NAD$^+$ following paclitaxel treatment was significantly higher ($p < 0.01$) than without it. However, neither 5 μM of LY-294002 (Fig. 7A) nor 5 μM of Akt inhibitor IV (Fig. 7B) affected the NAD$^+$ levels when applied alone or in combination with PJ-34 and paclitaxel. Similar effect was noted in HeLa cells (data not shown). Since the inhibition of PI-3K/Akt pathway did not interfere with the intracellular level of NAD$^+$ (Fig. 7) but significantly counteracted the effect of PARP inhibition on the cell viability compromised by paclitaxel administration (Fig. 6), reduction of NAD$^+$ depletion could not account for the paclitaxel resistance caused by the PARP inhibition, rather, PARP inhibition caused paclitaxel resistance was achieved by activating the PI-3K-Akt pathway to a very significant extent.

4. Discussion

It has been suggested that transient inhibition of DNA repair using potent PARP inhibitors could improve the efficacy of cancer treatments. Although more study is needed, recent reports demonstrated that the inhibition of poly(ADP-ribose) synthesis could selectively kill cancer cells when used for treating tumors with defective BRCA proteins [4,5]. These reports shed some light on the DNA-damage signaling and repair processes involving PARPs. Recently it has been proposed that, in addition to the effects on BRCA defective tumor cells, targeting specific DNA repair enzymes can open a new type of chemotherapeutic approach to malignant diseases. In particular, inhibitors of PARP-1 that sensitize cells to DNA-damaging agents are under extensive investigation [1,3]. It is well-documented that PARP-1 functions as a DNA-damage sensor that responds to both single and/or double strand DNA breaks (SSBs, DSBs), facilitating DNA repair and

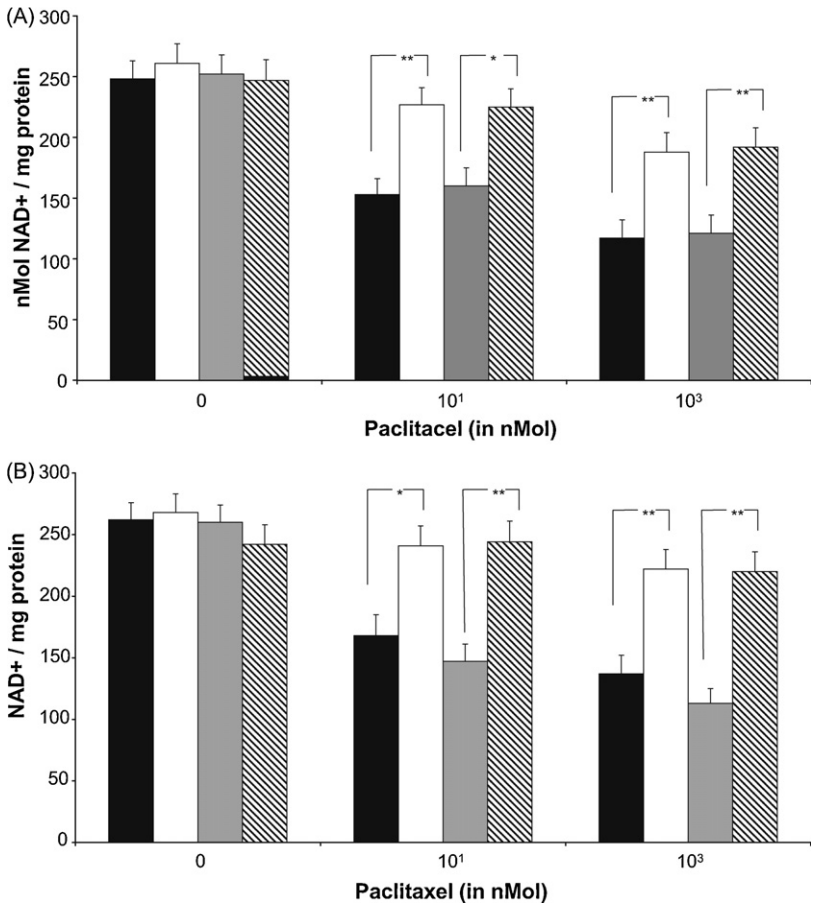

Fig. 7. Effect of PI3-K/Akt pathway inhibition on the intracellular NAD^+ content of paclitaxel treated cells. In (A) T24 cells were exposed for 24 h to different concentrations of paclitaxel alone (filled bars) or pretreated with 5 μM of LY-294002 (empty bars), with of 10 μM of PJ-34 (gray bars) or with the combination of PJ-34 and LY-294002 (striped bars). In (B) in an identical experimental setup, LY-294002 was replaced with 5 μM of Akt Inhibitor IV alone (empty bars) or in combination with PJ-34 (striped bars). Cellular NAD^+ levels were measured by the microplate version of the enzymatic cycling method using alcohol dehydrogenase. Data represent mean ± S.E.M. of three independent experiments running in four parallels. Note that the concentration axis is logarithmical. *, significant difference ($p < 0.05$); **, significant difference ($p < 0.01$) between cells treated with exposure to equimolar concentration of paclitaxel in the presence of PJ-34 alone and together with the Akt inhibitor.

cell survival. PARP-1, following binding to DNA, cleaves NAD^+ to ADP-ribose and nicotinamide and converts ADP-ribose into polymers of branched or linear poly(ADP-ribose) units (PAR) which can be attached to PARP-1 itself and to other nuclear acceptor proteins, including XRCC1, histones and so on [31,32]. These processes are important in the survival of the cells after extensive DNA damage but in normal cells the complete absence of PARP-1 protein or the inhibition of PARP-1 catalytic activity produces no significant growth defect [33]. This is supported by the observation that PARP-1 defective mice survive and have no obvious growth defect [34]. However, PARP-1 defective mice are more sensitive to high levels of high energy irradiation and to alkylating agents, showing that under some condition PARP-1 inactivation can facilitate cell death [35].

On the other hand, it is well-documented that, in response to extensive DNA damage, PARP-1 can be hyperactivated, eliciting activation of cell death by inducing signal transduction pathways [6–8], by direct mitochondrial damaging effect and can suppress the activity of the cytoprotective PI-3-kinase Akt pathway, and also can induce rapid cellular NAD^+ and ATP pool depletion resulting in necrotic or apoptotic cell death. PARP-1 hyperactivation has been documented in a number of pathological conditions including ischemia-reperfusion, myocardial infarction, and reactive oxygen species (ROS)-induced injury (2). In each case, inhibition of PARP-1 improved the survival of damaged cells or tissues [2,36,37]. In several cases, there are data showing that PARP-1 inhibition activated the PI-3-kinase–Akt pathway which can lead to cytostatic resistance [8,19–23], therefore PARP-1 inhibition depending on the precise conditions can facilitate, or inhibit, cell death.

In the present paper, we investigated the effect of PARP inhibition on the paclitaxel-induced cell death process using two different tumor cell lines. According to our data inhibition of PARP-1 significantly compromises the cell death inducing effect of paclitaxel, resulting in cytostatic resistance to a wide range of paclitaxel concentration (Figs. 2 and 3). This paclitaxel resistance was unlikely to be mediated by ABC transporter related mechanisms, since verapamil that blocks the P-glycoprotein pathway did not interfere with the desensitizing effect of PJ-34. Furthermore, we determined directly the interaction of PJ-34 and verapamil on taxol uptake of T24 cells by measuring the cellular paclitaxel concentrations after incubating the cells with paclitaxel in combination with PJ-34 and/or verapamil (Table 1). This experiment confirmed that ABC-transporter related mechanisms were not significantly involved in the paclitaxel resistance induced by PARP inhibition.

Although PJ-34 is a well-characterized PARP-1 inhibitor, the specificity of a small molecular weight synthetic inhibitor is always questionable because of the presence of several enzymes with poly- and mono-ADP-ribosylating activity in cells (1). Knocking down of PARP-1 in T24 cells by siRNA technique induced paclitaxel resistance (Fig. 3B) similar to that caused by PJ-34, indicating that PARP-1 protein played a significant role in this process, although the question remains as to whether the suppression of PARP-1 catalytic activity or the absence of PARP-1 protein was responsible

for the observed phenomenon. The transdominant expression of PARP-DBD inhibits ADP-ribosylation by PARP because binding to single-strand DNA breaks is essential for the activation of PARP-1, and the PARP-DBD competes with PARP-1 in binding to single-strand DNA breaks, and the former does not have catalytic activity. In a previous study, we demonstrated that PARP-DBD was localized almost exclusively to the nucleus [8], so it was clearly in position to compete with PARP-1. Transdominant expression of PARP-DBD induced paclitaxel resistance in tumor cells (Fig. 3A), which was similar to the effect caused by PJ-34. Since the design of the siRNA and the PARP-DBD was based on the sequence of nuclear PARP-1, it is unequivocal that the paclitaxel resistance was the consequence of the inhibition of the single-strand DNA break-induced PARP-1 activation, and was not due to the absence of PARP-1 protein or to another mechanism that might be regulated by the pharmacological inhibitor. However, since pharmacological PARP inhibitors are expected to be used in the clinical practice for supplementing anticancer agents, in the following experiments of our study we used a pharmacological agent in modeling the effect of PARP-1 inhibition.

In a previous report, we showed that PARP inhibition protected the mitochondrial membrane system, and this mechanism was significantly involved in its cytoprotective effect during oxidative stress [8]. We addressed the question of whether such a mechanism was involved in the PJ-34 induced paclitaxel resistance by comparing release of cytochrome *c* from the mitochondria to the cytosol and caspase-3 activation (Fig. 4) in response to paclitaxel treatment alone vs. in combination with PJ-34. We found that PJ-34 significantly decreased both hallmarks of apoptosis suggesting that the preservation of the mitochondrial membrane system indeed might be involved in the effects of the PARP inhibitor. We checked what kinase signaling pathways were activated by the paclitaxel treatment when applied alone or in combination with PJ-34. In agreement with the literature [17], paclitaxel treatment induced the activation of JNK, but it was not significantly affected by PJ-34 (Fig. 5). Several previous studies demonstrated that activation of the PI-3K-Akt system was strongly involved in mediating drug resistance under various conditions [19–23]. In accord with our previous data [8], PARP inhibition induced the phosphorylation and thus the activation of Akt which could phosphorylate and inactivate FOXO transcription factors [38] and so compromised the activation of the cell death process. In addition, Akt activation could protect mitochondrial membrane systems and could inactivate caspase-3 [39,8] therefore it is likely that PARP-1 inhibition-induced Akt activation plays a pivotal role in the resistance against taxol induced cell death.

The significance of Akt activation in PARP inhibition-induced paclitaxel resistance can be assessed by inhibiting Akt activation. When we blocked Akt activation either by inhibiting its upstream activator, the PI-3-kinase using LY-294002 or another upstream activator using Akt inhibitor IV, we observed significantly decreased PJ-34-induced paclitaxel resistance (Fig. 6). That is, Akt activation played a pivotal role in PARP inhibitor induced paclitaxel resistance. Although specificity and possible side-effects of a pharmacological agent is always an issue, LY 294002 has been reported to inhibit all isoforms of PI-3 kinase while not affecting other kinases such as PKC, PKA, MAP kinase, S6 kinase, EGF tyrosine kinase, c-src kinase, PI-4 kinase and diacylglycerol kinase [40]. Akt inhibitor IV has been less thoroughly characterized, but it was reported not to affect PI-3K, and to block Akt-mediated FOXO1a nuclear export and cell proliferation in 786-O cells [41]. Since two inhibitors of different chemical structure and targeting different upstream activators of Akt gave the same results, the effect of the aforementioned kinase inhibitors on the PARP inhibition-induced paclitaxel resistance was most likely due to their main pharmacological effect on their respective kinases rather than the result of a side-effect.

It is well-documented that FOXO1 and FOXO3 have a pro-apoptotic function in cell death processes and that FOXOs induce the overexpression of their downstream targets such as Fas ligand and Bim [14]. These processes and FOXO-dependent overexpression of the cell cycle inhibitor p27 (kip1) may be responsible for taxol-induced cell death [42,14]. NAD^+ depletion and induction of mitochondrial permeability transition were implicated as intermediate steps linking PARP-1 activation to mitochondrial cytochrome *c* release and consequent activation of the caspase pathway. We observed significant NAD^+ depletion in response to paclitaxel treatment that was significantly attenuated by PJ-34 (Fig. 7). It is worth mentioning that even when 1000 nM of paclitaxel was administered, a substantial amount of NAD^+ remained allowing the operation of ATP dependent cell functions, such as apoptotic processes and operation of kinase signaling pathways. However, and in contrast to the viability experiments, the PI-3K and Akt inhibitors did not counteract, in fact did not affect at all (Fig. 7), the protection of NAD^+ pool by PARP inhibition. This suggests that PI-3K and Akt activities are not involved in the regulation of intracellular NAD^+ level, and prevention of NAD^+ depletion by the PARP inhibitor did not play significant role in the PARP inhibition-induced paclitaxel resistance. Rather, activation of the PI-3K-Akt pathway was the significant factor in the drug resistance inducing effect of PARP inhibition, as described schematically in Fig. 8.

This study demonstrates that drug-induced drug resistance can be responsible for the reduced efficacy of antitumor treatment. The data show that although PARP-1 inhibition can facilitate cell death in cancer cells induced by DNA damaging agent, the effect of PARP-1 inhibition on the PI-3K-Akt signal transduction pathway could counteract this effect. Therefore, application of PARP inhibitors may represent a double-edged sword, which on the one hand, promotes cell death by inhibiting DNA repair while on the other hand, via activation of PI-3K/Akt pathway, promotes cell survival. This dual effect of PARP inhibition could be responsible for the contradictory data in this field [43–46]. It also suggests that to utilize the cell death promoting effect of PARP-1 inhibition in cancer therapy, the activation of PI-3k-Akt pathway should be suppressed by specific inhibitors.

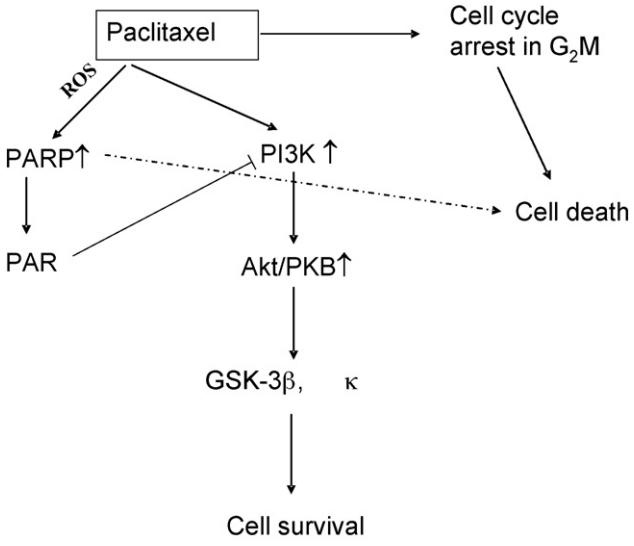

Fig. 8. Proposed molecular mechanism of the effect of PARP inhibition on paclitaxel resistance. Lines with *pointed ends* denote activation, whereas lines with *flat ends* indicate inhibition of the process. PARP-1 activation leads to NAD^+ consumption and by a yet unidentified mechanism to the inhibition of the PI3-kinase pathway leading to cells death. The inhibition of PARP-1 suppresses this process mainly via PI-3K/Akt activation resulting in increased cell survival.

Acknowledgments

This work was supported by grants from the Hungarian Science Foundation T 34320 as well as T 34307, from the Ministry of Health and Welfare ETT 35/2000, from PTE DD-KKK, and by grant NKFP 2001 1/026.

References

[1] Virag L, Szabo C. The therapeutic potential of poly(ADP-ribose) polymerase inhibitors. Pharmacol Rev 2002;54:375–429.
[2] Halmosi R, Berente Z, Osz E, Toth K, Literati-Nagy P, Sumegi B. Effect of poly(ADP-ribose) polymerase inhibitors on the ischemia-reperfusion-induced oxidative cell damage and mitochondrial metabolism in Langendorff heart perfusion system. Mol Pharmacol 2001;59:1497–505.
[3] Oliveira NG, Castro M, Rodrigues AS, Goncalves IC, Martins C, Toscano Rico JM, et al. Effect of poly(ADP-ribosyl)ation inhibitors on the genotoxic effects of the boron neutron capture reaction. Mutat Res 2005;583:36–48.
[4] De Soto JA, Wang X, Tominaga Y, Wang RH, Cao L, Qiao W, et al. The inhibition and treatment of breast cancer with poly (ADP-ribose) polymerase (PARP-1) inhibitors. Int J Biol Sci 2006;2:179–85.
[5] Bowman KJ, Newell DR, Calvert AH, Curtin NJ. Br J Cancer 2001;84:106–12.
[6] Veres B, Gallyas Jr F, Varbiro G, Berente Z, Osz E, Szekeres G, et al. Decrease of the inflammatory response and induction of the Akt/protein kinase B pathway by poly-(ADP-ribose) polymerase 1 inhibitor in endotoxin-induced septic shock. Biochem Pharmacol 2003;65:1115–28.
[7] Veres B, Radnai B, Gallyas Jr F, Varbiro G, Berente Z, Osz E, et al. Regulation of kinase cascades and transcription factors by a poly(ADP-ribose) polymerase-1 inhibitor, 4-hydroxyquinazoline, in lipopolysaccharide-induced inflammation in mice. J Pharm Exp Ther 2004;310:247–55.
[8] Tapodi A, Debreceni B, Hanto K, Bognar Z, Wittman I, Gallyas Jr F, et al. Pivotal role of Akt activation in mitochondrial protection and cell survival by poly(-ADP-ribose)polymerase-1 inhibition in oxidative stress. J Biol Chem 2005;280: 35767–75.
[9] Birkenkamp KU, Coffer PJ. FOXO transcription factors as regulators of immune homeostasis: molecules to die for? J Immunol 2003;171:1623–9.
[10] Torres K, Horwitz SB. Mechanisms of Taxol-induced cell death are concentration dependent. Cancer Res 1998;58:3620–6.
[11] Blagosklonny MV, Fojo T. Molecular effects of paclitaxel: myths and reality (a critical review). Int J Cancer 1999;83:151–6.
[12] Wang TH, Wang HS, Soong YK. Paclitaxel-induced cell death: where the cell cycle and apoptosis come together. Cancer 2000;88:2619–28.
[13] McDaid HM, Lopez-Barcons L, Grossman A, Lia M, Keller S, Perez-Soler R, et al. Enhancement of the therapeutic efficacy of taxol by the mitogen-activated protein kinase kinase inhibitor CI-1040 in nude mice bearing human heterotransplants. Cancer Res 2005;65:2854–60.
[14] Sunters A, Fernandez de Mattos S, Stahl M, Brosens JJ, Zoumpoulidou G, Saunders CA, et al. FoxO3a transcriptional regulation of Bim controls apoptosis in paclitaxel-treated breast cancer cell lines. J Biol Chem 2003;278:49795–805.
[15] Boehmerle W, Splittgerber U, Lazarus MB, McKenzie KM, Johnston DG, Austin DJ, et al. Paclitaxel induces calcium oscillations via an inositol 1,4,5-trisphosphate receptor and neuronal calcium sensor 1-dependent mechanism. Proc Natl Acad Sci USA 2006;103:18356–61.
[16] Varbiro G, Veres B, Gallyas Jr F, Sumegi B. Direct effect of Taxol on free radical formation and mitochondrial permeability transition. Free Rad Biol Med 2001;31:548–58.
[17] Sunters A, Madureira PA, Pomeranz KM, Aubert M, Brosens JJ, Cook SJ, et al. Paclitaxel-induced nuclear translocation of FOXO3a in breast cancer cells is mediated by c-Jun NH2-terminal kinase and Akt. Cancer Res 2006;66:212–20.
[18] Van Der Heide LP, Hoekman MF, Smidt MP. The ins and outs of FoxO shuttling: mechanisms of FoxO translocation and transcriptional regulation. Biochem J 2004;380:297–309.
[19] VanderWeele DJ, Zhou R, Rudin CM. Akt up-regulation increases resistance to microtubule-directed chemotherapeutic agents through mammalian target of rapamycin. Mol Cancer Ther 2004;3:1605–13.
[20] Priulla M, Calastretti A, Bruno P, Amalia A, Paradiso A, Canti G, et al. Preferential chemosensitization of PTEN-mutated prostate cells by silencing the Akt kinase. Prostate 2007;67:782–9.
[21] Asnaghi L, Calastretti A, Bevilacqua A, D'Agnano I, Gatti G, Canti G, et al. Bcl-2 phosphorylation and apoptosis activated by damaged microtubules require mTOR and are regulated by Akt. Oncogene 2004;23:5781–91.
[22] Clark AS, West K, Streicher S, Dennis PA. Constitutive and inducible Akt activity promotes resistance to chemotherapy, trastuzumab, or tamoxifen in breast cancer cells. Mol Cancer Ther 2002;1:707–17.
[23] Bevilacqua A, Ceriani MC, Canti G, Asnaghi L, Gherzi R, Brewer G, et al. Bcl-2 protein is required for the adenine/uridine-rich element (ARE)-dependent degradation of its own messenger. J Biol Chem 2003;278: 23451–9.
[24] Luhn P, Wang H, Marcus AI, Fu H. Identification of FAKTS as a novel 14-3-3-associated nuclear protein. Proteins 2007;67:479–89.
[25] Kim JW, Won J, Shon S, Joe CO. DNA-binding activity of the N-terminal cleavage product of poly(ADP-ribose) polymerase is required for UV mediated apoptosis. J Cell Sci 2000;113:955–61.
[26] Varbiro G, Toth A, Tapodi A, Veres B, Gallyas F, Sumegi B. Concentration dependent mitochondrial effect of amiodarone. Biochem Pharmacol 2003;65:1115–28.
[27] Kalai T, Varbiro G, Bognar Z, Palfi A, Hanto K, Bognar B, et al. Synthesis and evaluation of the permeability transition inhibitory characteristics of paramagnetic and diamagnetic amiodarone derivatives. Bioorg Med Chem 2005;13:2629–36.
[28] Shah GM, Poirier D, Duchaine C, Brochu G, Desnoyers S, Lagueux J, et al. Methods for biochemical study of poly(ADP-ribose) metabolism in vitro and in vivo. Anal Biochem 1995;227:1–13.
[29] Varbiro G, Toth A, Tapodi A, Veres B, Sumegi B, Gallyas Jr F. Protective effect of amiodarone but not N-desethylamiodarone on postischemic hearts through the inhibition of mitochondrial permeability transition. J Pharm Exp Ther 2003;307:615–25.
[30] Bognar Z, Kalai T, Palfi A, Hanto K, Bognar B, Szabo Z, et al. A novel SOD-mimetic permeability transition inhibitor agent protects ischemic heart by inhibiting both apoptotic and necrotic cell death. Free Rad Biol Med 2006;41:835–48.
[31] Jagtap P, Soriano FG, Virag L, Liaudet L, Mabley J, Szabo E, et al. Novel phenanthridinone inhibitors of poly (adenosine 5′-diphosphate-ribose) synthetase: potent cytoprotective and antishock agents. Crit Care Med 2002;30:1071–82.
[32] Keil C, Grobe T, Oei SL. MNNG-induced cell death is controlled by interactions between PARP-1, poly(ADP-ribose) glycohydrolase, and XRCC1. J Biol Chem 2006;218:34394–405.
[33] Tentori L, Lacal PM, Muzi A, Dorio AS, Leonetti C, Scarsella M, et al. Poly(ADP-ribose) W polymerase (PARP) inhibition or PARP-1 gene deletion reduces angiogenesis. Eur J Cancer 2007;43:2124–33.
[34] Oliver FJ, Menissier-de Murcia J, Nacci C, Decker P, Andriantsitohaina R, Muller S, et al. Resistance to endotoxic shock as a consequence of defective NF-kappaB activation in poly (ADP-ribose) polymerase-1 deficient mice. EMBO J 1999;18:4446–54.
[35] Wesierska-Gadek J, Gueorguieva M, Schloffer D, Uhl M, Wojciechowski J. Non-apoptogenic killing of hela cervical carcinoma cells after short exposure to the alkylating agent *N*-methyl-*N*′-nitro-*N*-nitrosoguanidine (MNNG). J Cell Biochem 2003;89:1222–34.
[36] Wang SJ, Wang SH, Song ZF, Liu XW, Wang R, Chi ZF. Poly(ADP-ribose) polymerase inhibitor is neuroprotective in epileptic rat via apoptosis-inducing factor and Akt signaling. Neuroreport 2007;18:1285–9.
[37] Pacher P, Cziraki A, Mabley JG, Liaudet L, Papp L, Szabo C. Role of poly(ADP-ribose) polymerase activation in endotoxin-induced cardiac collapse in rodents. Biochem Pharmacol 2002;64:1785–91.
[38] Burgering BM, Kops GJ. Cell cycle and death control: long live Forkheads. Trends Biochem Sci 2002;27:352–60.
[39] Zhang HM, Rao JN, Guo X, Liu L, Zou T, Turner DJ, et al. Akt kinase activation blocks apoptosis in intestinal epithelial cells by inhibiting caspase-3 after polyamine depletion. J Biol Chem 2004;279:22539–47.
[40] Vlahos CJ, Matter WF, Hui KY, Brown RF. A specific inhibitor of phosphatidylinositol 3-kinase, 2-(4-morpholinyl)-8-phenyl-4H-1-benzopyran-4-one (LY294002). J Biol Chem 1994;269:5241–8.
[41] Kau TR, Schroeder F, Wojciechowski CL, Zhao JJ, Roberts TM, Clardy J, et al. A chemical genetic screen identifies inhibitors of regulated nuclear export of a Forkhead transcription factor in PTEN-deficient tumor cells. Cancer Cell 2003;4:463–76.
[42] Trotman LC, Alimonti A, Scaglioni PP, Koutcher JA, Cordon-Cardo C, Pandolfi PP. Identification of a tumour suppressor network opposing nuclear Akt function. Nature 2006;441:523–7.
[43] de Soto JA, Deng CX. PARP-1 inhibitors: are they the long-sought genetically specific drugs for BRCA1/2-associated breast cancers? Int J Med Sci 2006;3:117–23.
[44] Gallmeier E, Kern SE. Absence of specific cell killing of the BRCA2-deficient human cancer cell line CAPAN1 by poly(ADP-ribose) polymerase inhibition. Cancer Biol Ther 2005;4:703–6.
[45] Bryant HE, Helleday T. Poly(ADP-ribose) polymerase inhibitors as potential chemotherapeutic agents. Biochem Soc Trans 2004;32:959–61.
[46] Malanga M, Althaus FR. The role of poly(ADP-ribose) in the DNA damage signaling network. Biochem Cell Biol 2005;83:354–64.